Apg13p and Vac8p are part of a complex of phosphoproteins that are required for cytoplasm to vacuole targeting

Scott, SV; Nice, DC; Nau, JJ; Weisman, LS; Kamada, Y; Keizer-Gunnink, [No Value]; Funakoshi, T; Veenhuis, M; Ohsumi, Y; Klionsky, DJ

Published in:
The Journal of Biological Chemistry

DOI:
10.1074/jbc.M002813200

Publication date:
2000

THE JOURNAL OF BIOLOGICAL CHEMISTRY
Vol. 275, No. 33, Issue of August 18, pp. 25840–25849, 2000

Printed in U.S.A.

Apg13p and Vac8p Are Part of a Complex of Phosphoproteins That Are Required for Cytoplasm to Vacuole Targeting*

Received for publication, April 3, 2000, and in revised form, May 31, 2000
Published, JBC Papers in Press, June 2, 2000, DOI 10.1074/jbc.M002813200

Sidney V. Scott‡§, Daniel C. Nice III‡§, Johnathan J. Nau¶, Lois S. Weisman¶, Yoshiaki Kamada‖, Ineke Keizer-Gunnink, Tomoko Funakoshi‖ ‡‡, Marten Veenhuis**, Yoshinori Ohsumi‖, and Daniel J. Klionsky‡ §§**

*From the ‡Section of Microbiology, University of California, Davis, California 95616, the ¶Department of Biochemistry, University of Iowa, Iowa City, Iowa 52242, the **Department of Microbiology, University of Groningen, NL-9751 NN Haren, The Netherlands, and the ‖Department of Cell Biology, National Institute for Basic Biology, Okazaki 444-8585, Japan*

We have been studying protein components that function in the cytoplasm to vacuole targeting (Cvt) pathway and the overlapping process of macroautophagy. The Vac8 and Apg13 proteins are required for the import of aminopeptidase I (API) through the Cvt pathway. We have identified a protein-protein interaction between Vac8p and Apg13p by both two-hybrid and co-immunoprecipitation analysis. Subcellular fractionation of API indicates that Vac8p and Apg13p are involved in the vesicle formation step of the Cvt pathway. Kinetic analysis of the Cvt pathway and autophagy indicates that, although Vac8p is essential for Cvt transport, it is less important for autophagy. *In vivo* phosphorylation experiments demonstrate that both Vac8p and Apg13p are phosphorylated proteins, and Apg13p phosphorylation is regulated by changing nutrient conditions. Although Apg13p interacts with the serine/threonine kinase Apg1p, this protein is not required for phosphorylation of either Vac8p or Apg13p. Subcellular fractionation experiments indicate that Apg13p and a fraction of Apg1p are membrane-associated. Vac8p and Apg13p may be part of a larger protein complex that includes Apg1p and additional interacting proteins. Together, these components may form a protein complex that regulates the conversion between Cvt transport and autophagy in response to changing nutrient conditions.

The majority of intracellular degradation is carried out in the lysosome/vacuole of eukaryotic cells. In order to compartmentalize these reactions, substrates as well as degradative enzymes must be faithfully delivered to this organelle. In *Saccharomyces cerevisiae*, proteins are known to be delivered to the vacuole for degradation by several different pathways (1). For example, cell surface proteins are transported by endocytosis; the cytosolic enzyme fructose-1,6-bisphosphatase is targeted to the vacuole by the vacuolar import and degradation pathway when changing nutrient conditions necessitate down-regulation; and during periods of starvation, bulk cytosol is packaged into vesicles and delivered to the vacuole by macroautophagy. Vacuole resident proteins are delivered by four characterized pathways. In the carboxypeptidase Y pathway, proteins travel through the secretory pathway and are diverted from the late Golgi to the vacuole via an endosomal intermediate or prevacuolar compartment (PVC).[1] The multivesicular body sorting pathway also utilizes the PVC, but in this case proteins enter vesicles resulting from invagination of the organelle's limiting membrane. The alkaline phosphatase (ALP) pathway utilizes the early secretory compartments, but the proteins are transported from the late Golgi to the vacuole without passing through the PVC. In the cytoplasm to vacuole targeting (Cvt) pathway, cargo is packaged into cytosolic vesicles that are delivered to the vacuole.

Under vegetative conditions the yeast vacuolar hydrolase aminopeptidase I (API) is targeted to the vacuole by the Cvt pathway. API is synthesized as a precursor in the cytosol where it rapidly oligomerizes into dodecamers (2). Multiple API dodecamers then assemble into a membrane-bound complex called a Cvt complex (3). Double membrane structures surround the Cvt complex resulting in the formation of Cvt vesicles. The outer membrane of these vesicles fuses with the vacuole resulting in the release of a still intact vesicle, called a Cvt body, into the vacuole lumen. These structures are broken down by resident hydrolases, and the released precursor API (prAPI) is processed to its mature size.

Yeast mutants have been isolated that are defective in the Cvt pathway (4, 5). Analysis of these mutants revealed that many are allelic to mutants in macroautophagy (*apg* and *aut*; Refs. 5–8). This was a surprising finding because the transport of prAPI is selective and constitutive, while delivery of soluble cytosolic proteins to the vacuole by macroautophagy is nonselective and is induced by stress conditions such as starvation (5). However, it is worth noting that under certain conditions macroautophagy may be a selective process. For example, peroxisomes can be selectively degraded by a macroautophagic process in response to changing nutrient conditions (reviewed in Ref. 9).

* This work was supported by National Institutes of Health Public Health Service Grants GM53396 (to D.J.K.) and GM50403 (to L.S.W.), an American Cancer Society Senior Postdoctoral Fellowship (to S.V.S.) and Grants-in-Aid for Scientific Research from the Ministry of Education, Science, and Culture of Japan (to Y.O.). The costs of publication of this article were defrayed in part by the payment of page charges. This article must therefore be hereby marked "*advertisement*" in accordance with 18 U.S.C. Section 1734 solely to indicate this fact.

§ These authors contributed equally to this work.

‡‡ Present address: Dept. of Biochemistry, College of Pharmacy, Nihon University, Funabashi, Chiba 274-8555 Japan.

§§ To whom correspondence should be addressed. Tel.: 530-752-0277; Fax: 530-752-9014; E-mail: djklionsky@ucdavis.edu.

[1] The abbreviations used are: PVC, prevacuolar compartment; ALP, alkaline phosphatase; API, aminopeptidase I; Arm, armadillo repeat; Cvt, Cytoplasm to vacuole targeting; PGK, phosphoglycerate kinase; PrA, proteinase A; SD-N, synthetic minimal medium lacking nitrogen; SMD, synthetic minimal medium containing nitrogen; NPM, low phosphate medium; prAPI, precursor aminopeptidase I; kb, kilobase pair(s); GFP, green fluorescent protein; PCR, polymerase chain reaction; PIPES, 1,4-piperazinediethanesulfonic acid.

TABLE I
Yeast strains used in this study

Strain	Genotype	Source or reference
SEY6210	*MATα leu2–3,112 ura3–52 his3-Δ200 trp1-Δ901 lys2–801 suc2-Δ9 GAL*	(41)
BJ2168	*MATa prb1–1122 prc1–407 pep4–3 leu2 trp1 ura3–52 gal2*	(42)
LWY7235	*MATa leu2–3,112 ura3–52 his3-Δ200 trp1-Δ901 lys2–801 suc2-Δ9*	(12)
TN121	*MATa leu2–3,112 trp1 ura3–52 pho8::pho8Δ60 pho13::URA3*	(36)
TN124	*MATa leu2–3,112 trp1 ura3–52 pho8::pho8Δ60 pho13::LEU2*	(36)
NNY20	*MATa ura3 trp1 leu2 apg1Δ::LEU2*	(28)
TVY1	*MATα leu2–3,112 ura3–52 his3-Δ200 trp1-Δ901 lys2–801 suc2-Δ9 GAL pep4Δ::LEU2*	(43)
AHY001	*SEY6210 cvt9Δ::HIS3*	This study
D3Y101	*LWY7235 apg13Δ::LEU2*	This study
D3Y102	*SEY6210 vac8Δ::TRP1*	This study
D3Y103	*TN124 apg13Δ::URA3*	This study
D3Y104	*TN121 vac8Δ::TRP1*	This study
D3Y105	*D3Y101 pep4Δ::URA3*	This study
D3Y106	*TVY1 vac8Δ::TRP1*	This study

Biochemical and morphological studies confirm that the basic properties of targeting by the Cvt pathway are similar to those of macroautophagy (3, 10). Both pathways involve formation of double membrane vesicles that engulf cytosolic cargo and deliver it to the vacuole by fusion of the outer membrane with the vacuole surface. When cells are growing in rich media, the primary mode of prAPI delivery is via Cvt vesicles (3). These vesicles are approximately 150 nm in diameter, relatively rare, and contain concentrated cargo that appears different than bulk cytosol. In contrast, in starvation conditions, the majority of prAPI appears to be targeted to the vacuole by autophagosomes. Compared with Cvt vesicles, autophagosomes are larger (approximately 300–900 nm), more abundant, and appear to contain bulk cytosolic components in addition to Cvt complexes. The mechanisms by which environmental changes are transduced to signal alterations in vesicle morphology and selectivity are not known. Recent cloning of the genes that complement mutants defective in the autophagy and Cvt pathways indicates that the majority of the molecular components involved in these pathways are shared (reviewed in Ref. 9). However, several mutants have been identified that appear to be defective primarily in one or the other of these pathways. These include *aut4* (6), *apg17*,[2], *cvt3* (5), *cvt9*,[3] *tlg2* (11), and *vac8* (12).

The *vac8* mutant was identified through a screen for strains defective in vacuole inheritance (13). In addition to a role in the migration of vacuoles from the mother to the bud during cell division, Vac8p is required for Cvt transport. Analysis of *vac8* mutants by a vesicle test that monitors the accumulation of subvacuolar vesicles under starvation conditions, however, provided preliminary evidence that this protein is not necessary for autophagy (12). The majority of Vac8p consists of 11 armadillo repeats. These domains are contained within the *Drosophila* armadillo protein and the mammalian homologues β-catenin and plakoglobin. The armadillo domains in β-catenin and plakoglobin serve to link regions of the plasma membrane to actin, and Vac8p co-sediments with actin filaments *in vitro* (12). Localization experiments indicate that Vac8p is found primarily on the vacuole membrane (12, 14, 15). In addition, Vac8p is both myristoylated and palmitoylated, and mutational analysis indicates that acylation is required both for vacuole localization of Vac8p and for vacuole inheritance. Interestingly, *vac8* mutants defective in acylation are not defective in Cvt transport, suggesting that different cellular pools of Vac8p are utilized for inheritance and Cvt transport (12).

To identify proteins that interact with Vac8p, we have performed a two-hybrid screen using this protein as bait. We identified Apg13p as a Vac8p-interacting protein. Apg13p is predicted to be an 83-kDa protein, with no significant homology to other known proteins (16). Overexpression of *APG1* suppresses the autophagy defect in the *apg13–1* mutant, suggesting that these two proteins also interact (16). Mutants in *APG13* are defective in both the Cvt and autophagy pathways (5, 16). We propose that these proteins are part of a large protein complex that functions in the vesicle formation step that is required for sequestration of cargo during import from the cytoplasm to the vacuole.

EXPERIMENTAL PROCEDURES

Strains and Media—The *S. cerevisiae* strains used in this study are listed in Table I.

Yeast strains were grown in the indicated media: synthetic minimal medium (SMD; 0.67% yeast nitrogen base, 2% glucose, and auxotrophic amino acids and vitamins as needed), YPD (1% yeast extract, 2% peptone, 2% glucose), synthetic minimal medium containing 2% glucose without ammonium sulfate or amino acids (SD-N), and low phosphate medium (NPM; 2% glucose, 0.5% casamino acids, 1× complete amino acid mix, 1% proline, 2 mM NaCl, 4 mM $MgCl_2$).

Reagents—Restriction endonucleases and DNA modifying enzymes were from New England Biolabs (Beverly, MA). Proteinase K and complete EDTA-free protease inhibitor mixture were from Roche Molecular Biochemicals. Antiserum to proteinase A (PrA), ALP, and Vac8p were described previously (12, 17, 18). Antiserum to Apg13p and Cvt9p were generated as described.[2,3] Antiserum to phosphoglycerate kinase (PGK) was generously provided by Dr. Jeremy Thorner (19). Monoclonal antibodies to the hemagglutinin epitope were from Covance Research Products (Richmond, CA). Horseradish peroxidase-conjugated anti-rabbit goat antibody was from Jackson ImmunoResearch Laboratories, Inc. (West Grove, PA). ECL reagents were from Amersham Pharmacia Biotech. EXPRE^{35}S^{35}S protein-labeling mix and [^{33}P]orthophosphate were from NEN Life Science Products. Oxalyticase was from Enzogenetics (Corvallis, OR) and Zymolyase 100T from Seikagaku Kogyo (Tokyo, Japan). Immobilon-P (polyvinylidene fluoride) was from Millipore Corp. (Bedford, MA). Plasmid pTrcHisB was from Invitrogen (Carlsbad, CA). Antiserum to Apg1p and additional antiserum to Apg13p were generated as follows: Synthetic peptides corresponding to amino acids 105–123 and 643–664 of Apg1p and amino acids 613–633 and 715–726 of Apg13p were conjugated to keyhole limpet hemocyanin (Multiple Peptide Systems, San Diego, CA) and injected into New Zealand White rabbits. All other reagents were from Sigma.

Constructs and Two-hybrid Analysis—The plasmid pCuCvt9 expressing the *CVT9* gene under control of the regulable *CUP1* promoter will be described elsewhere.[3] Plasmid pYK128 contains the *APG1* gene with an N-terminal 3xHA epitope tag cloned into the vector pRS423, pYW10 contains *VAC8* cloned into pRS426 (12) and YEp351(APG13) contains the *APG13* gene cloned into the YEp351 plasmid.[2] The following plasmids encode *VAC8* bearing deletions in the indicated armadillo repeat domains: pLT4, ΔArm1; pLT5, ΔArm2; pLT6, ΔArm3; pYWT1,

[2] Y. Kamada, T. Funakoshi, T. Shintani, K. Nagano, M. Ohsumi, and Y. Ohsumi, submitted for publication.
[3] J. Kim, J. Guan, Y. Kamada, A. Hefner-Gravink, Y. Ohsumi, and D. J. Klionsky, manuscript in preparation.

ΔArm4–7[4]; and pYW51, ΔArm1–3 (12).

APG13 was amplified from strain SEY6210 genomic DNA into two overlapping fragments by two PCR reactions. For reaction one, the sense primer was 5′-CGCGTCAGAGCAAGAGGTGAAAGGGTTGCCACGTA-3′ and the antisense primer was 5′-GTGGCCCGTAGTTGGAGCTCATACTTGGCC-3′. For reaction two, the sense primer was 5′-GTCTATCCAATATCGAGACCTGTTCAACCA-3′ and the antisense primer was 5′-GGAAACGCAGTCAGCGGGTGACAAATAAGC-3′. Utilizing the overlapping fragments as a template, the *APG13* coding region was PCR-amplified with the primers 5′-GTTGAATAGCTGCAGTCCTGGTTGCCGAAG-3′, which adds a *Pst*I site, and 5′-TAAAATAAAAGCTTACCATTTTTA-3′, which adds a *Hin*dIII site. The amplified fragment was inserted into the *Pst*I and *Hin*dIII sites of pTrcHisB to generate pTrcHisBAPG13.

Construction of the VAC8 Two-hybrid Bait Plasmid—The *VAC8* coding region was PCR-amplified with the primers V22 (5′-CATGCCATGGTGGGTTCATGTTGTAGTTGC-3′), which adds a *Nco*I site and V23 (5′-ACGCGTCGACTCAATGTAAAAATTGTAAAATCTGTTG-3′), which adds a *Sal*I site. *Nco*I-*Sal*I-digested *VAC8* was cloned into *Nco*I-*Sal*I-digested pAS2 (20) to create the *VAC8* two-hybrid bait plasmid pYW31. The same strategy was used to clone the mutated *vac8* gene from pLT4, pLT5, pLT6, pYWT1, and pYW51 into the two-hybrid vector.

Two-hybrid Library Screen—The bait plasmid pYW31 was transformed into the yeast strain PJ69-4A (21) and checked for activation of the reporter genes. The resulting strain PJ69-4A + pYW31 was transformed with the two-hybrid yeast library pool Y2HL-C1 (21). Approximately 280,000 transformants were screened. The transformants were plated onto SC-His-Leu-Trp + 3 mM 3-amino-1,2,4-triazole and incubated at 24 °C for 14 days. These plates were replica plated onto SC-Ade-Leu-Trp and incubated at 24 °C for 5 days. Colonies were picked and tested for β-galactosidase activity. Library plasmids were isolated from the yeast strain and retransformed into PJ69-4A + pYW31. Plasmids that showed positive responses after retransformation were sequenced and identified by comparison with the *Saccharomyces* Genome Data base. Two identical clones of *APG13* that coded for amino acids 567–738 were isolated.

Construction of the APG13 Two-hybrid Prey Plasmids—Plasmid pTrcHisBAPG13 was digested with *Pst*I and *Hin*dIII. The 2.2-kb *APG13* fragment was cloned into *Pst*I-*Hin*dIII-cut pBlueScript SK to create pJN21. The following plasmids were generated by digesting pJN21 with the indicated enzymes, isolating DNA of the size noted, and ligating into pGAD-C (1–3) that had been digested with the indicated enzymes to construct prey plasmids encoding the indicated number of amino acids of Apg13p: pJN22 (pADAPG13), *Sal*I and partially digested with *Bam*HI (2.2 kb), into *Bam*HI-*Sal*I sites of C2, full-length Apg13p; pJN23 (pAD1–520APG13), *Bam*HI (1.6 kb), into *Bam*HI sites of C2, amino acids 1–520; pJN24 (pAD1–279APG13), *Bam*HI-*Nsi*I (0.8 kb), into *Bam*HI-*Pst*I sites of C2, amino acids 1–279; pJN25 (pAD280–520APG13), *Nsi*I-*Bam*HI (0.8 kb), into *Pst*I-*Bgl*II sites of C2, amino acids 280–520; pJN26 (pAD280–714APG13), *Nsi*I (1.3 kb), into *Pst*I sites of C2, amino acids 280–714; pJN27 (pAD521–738APG13), *Bam*HI-*Sal*I (0.7 kb), into *Bam*HI-*Sal*I sites of C3, amino acids 521–738; pJN28 (pAD521–692APG13), *Bam*HI-*Cla*I (0.5 kb), into *Bam*HI-*Cla*I sites of C3, amino acids 521–692; pJN29 (pAD693–738APG13), *Cla*I-*Sal*I (0.2 kb), into *Cla*I-*Sal*I sites of C1, amino acids 692–738.

Control plasmids for the two-hybrid analysis were pSE1111 containing *SNF4* fused to the *GAL4* activation domain in pACT and pSE1112 containing *SNF1* fused to the *GAL4* binding domain in pAS1 (22).

Subcellular Fractionation—Yeast strains were grown to an A_{600} = 0.8–1, and converted to spheroplasts as described (23). *vac8*Δ cells were grown in SMD, and *apg13*Δ cells were grown in YPD. Spheroplasts were washed in PS1000 (20 mM K-PIPES, pH 6.8, 1 M sorbitol), and subjected to osmotic lysis (23) by pipetting up and down 10 times in PS200 with $MgCl_2$ (20 mM K-PIPES, pH 6.8, 200 mM sorbitol, 5 mM $MgCl_2$) at a cell concentration of 20 A_{600}/ml. The supernatant and pellet fractions were collected after centrifugation at 5000 × *g* for 5 min. A flotation analysis was carried out as described previously (23). The pellet fraction was resuspended in 100 μl of 15% Ficoll, and then overlaid with 1 ml of 13% Ficoll and 300 μl of 2% Ficoll. The resulting step gradients were subjected to centrifugation in a microcentrifuge at 12,000 × *g* for 10 min. The float fraction was collected from the 2% Ficoll/13% Ficoll interface. Proteinase K treatment was with 50 μg of proteinase K for 15 min on ice with a concentration of osmotically lysed spheroplasts equivalent to 20 A_{600}/ml. All fractions were precipitated with trichloroacetic acid, resolved by SDS-polyacrylamide gel electrophoresis, and subjected to immunoblotting as described (4).

Fractionation of Apg13p and Apg1p was as above except that the isolated spheroplasts were washed with PS1000 with complete EDTA-free protease inhibitor mixture before lysis and then lysed in PS200 with 5 mM $MgCl_2$ and protease inhibitors. The pellet fraction was collected by centrifugation at 13,000 × *g* for 5 min at 4 °C.

Pulse-Chase Labeling Analysis—Pulse labeling experiments were as described (5). Yeast strains were grown in SMD medium to an A_{600} = 0.8–1, pelleted, and then pulse-labeled at 30 °C in fresh SMD with 11 μCi/A_{600} Expre^{35}S^{35}S label. Chase reactions were initiated by addition of 10 μM cysteine and 20 μM methionine. Cells were then pelleted and resuspended at a concentration of 1 A_{600}/ml in either SMD or SD-N for the duration of the chase reaction. API was immunoprecipitated as described (24).

Electron Microscopy—Indicated yeast strains were grown in YPD to an A_{600} = 1, harvested, washed, incubated in SD-N for 4 h, and fixed with 1.5% $KMnO_4$ as described (25).

Phosphate Labeling—Cells were grown to an A_{600} of 0.5–1 in NPM. 4 A_{600} units of cells were harvested and labeled for 30 min at 30 °C in 100 μl of fresh NPM with 25 μCi of [^{33}P]orthophosphate. Cells were recovered by centrifugation, and proteins were precipitated with 10% trichloroacetic acid and subjected to immunoprecipitation as described previously (24), except that single precipitation reactions were performed.

Co-immunoprecipitation Experiments—BJ2168 cells harboring pYW10 and YEp351(APG13) were grown in 100 ml of YPD, collected by centrifugation, washed with water, and resuspended in 50 ml of Z buffer (50 mM Tris-HCl pH7.5, 1 M sorbitol, 1% yeast extract, 2% peptone, 1% glucose) containing 0.5 mg/ml Zymolyase 100T. The suspension was incubated for 40 min at 30 °C with gentle shaking to generate spheroplasts. The resultant spheroplasts were washed once with Z buffer, resuspended in 50 ml of Z buffer, and divided into two 25-ml aliquots. Rapamycin (0.4 μg/ml, prepared in 90% ethanol, 10% Triton X-100) was added to one aliquot, and the spheroplasts were incubated for 1 h at 30 °C with gentle shaking. The spheroplasts were collected and washed with 50 mM Tris-HCl, pH 7.5, 1 M sorbitol, and lysed by suspending in 1 ml of lysis buffer (phosphate-buffered saline, pH 7.4, 1 mM EDTA, 1 mM EGTA, 2 mM Na_3VO_4, 50 mM KF, 15 mM sodium pyrophosphate, 15 mM *p*-nitrophenylphosphate, 20 μg/ml leupeptin, 20 μg/ml benzamidine, 10 μg/ml pepstatin A, 40 μg/ml aprotinin, 1 mM phenylmethylsulfonyl fluoride, and 0.5% Tween 20). The cell lysate was further incubated on ice for 5 min, and spun down at 6,500 rpm for 10 min at 4 °C to remove cell debris. The resultant supernatant was collected and incubated with 20 μl of protein G-Sepharose (50% suspension) for 30 min at 4 °C with gentle agitation. The cell lysate was spun down, and the supernatant (two 500-μl aliquots) was incubated with or without 2 μl of anti-Vac8p serum for 1.5 h at 4 °C with gentle agitation. 20 μl of protein G-Sepharose (50% suspension) was added to the lysate/antiserum mixture, followed by further incubation for 1.5 h at 4 °C with gentle agitation. The immune complex was washed three times with lysis buffer, and the resulting immunocomplex was subjected to immunoblotting using anti-Apg13p antibody (1:5,000 dilution) or anti-Vac8p antibody (1:5,000 dilution). For secondary antibody, horseradish peroxidase-conjugated anti-rabbit goat antibody (1:10,000) was used. Immunodetection was carried out with the ECL system.

RESULTS

Vac8p and Apg13p Interact—The *vac8* mutant was identified in a screen for strains defective in vacuolar inheritance (13). Vac8p is unusual among those proteins involved in organelle segregation in that it was also found to be required for the import of the resident vacuolar hydrolase aminopeptidase I through the cytoplasm to vacuole targeting pathway. To gain further information on the role of Vac8p in the Cvt pathway, a two-hybrid screen was used to identify proteins that interact with Vac8p. The *VAC8* gene was cloned into a two-hybrid vector containing a DNA-binding domain. A *his3 ade2* strain was transformed with the resulting pBD-VAC8 plasmid and a plasmid library that had been cloned into the transcriptional activating domain vector. Transformants were screened for growth on His-free plates, and then growth on Ade-free plates and finally for β-galactosidase activity. Plasmids were recovered from cells that were positive by all three criteria and were subjected to DNA sequencing. One of the genes that was iden-

[4] F. Tang, J. Nau, E. Kauffman, and L. Weisman, manuscript in preparation.

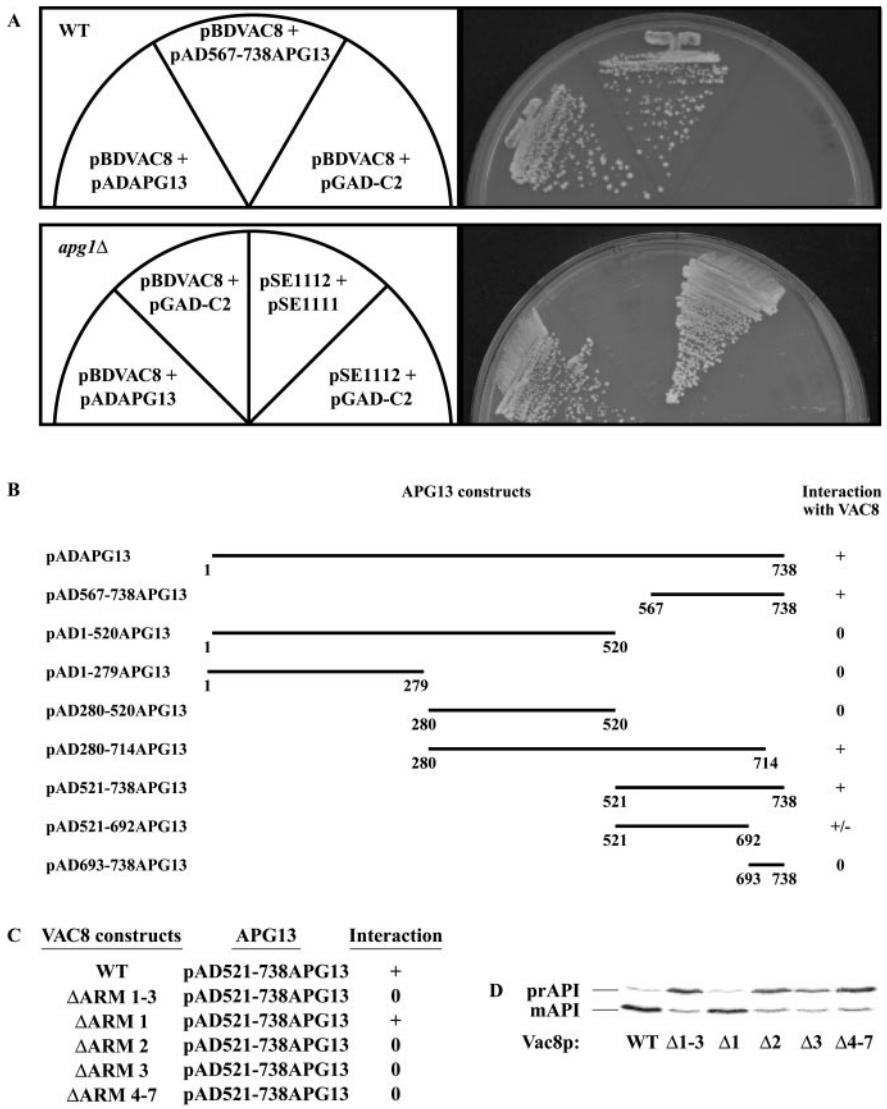

FIG. 1. **Two-hybrid interaction identifies Apg13p as a protein that interacts with Vac8p.** *A*, growth on SC-Ade-His-Trp-Leu + 3 mM 3-amino-1,2,4-triazole after 5 days at 24 °C. Plasmids transformed into PJ69-4A (*WT*) and the corresponding *apg1*Δ strains are indicated. Vac8p interacts with full-length Apg13p in both wild type and *apg1*Δ strains. *B*, growth on SC-Ade-His-Trp-Leu + 3 mM 3-amino-1,2,4-triazole. PJ69-4A was transformed with pYW31 (*VAC8*) and the *APG13* constructs indicated. *Numbers* indicate the amino acids of Apg13p. + indicates growth after 5 days at 24 °C. *0* indicates no growth after 5 days at 24 °C. +/− indicates slight growth after 12 days at 24 °C. *C*, Arm domains in Vac8p are required for Apg13p interaction. Strain PJ69-4A was transformed with pAD521–738APG13 and binding domain plasmids containing either wild type *VAC8* (*WT*), or arm deletions of *VAC8* as indicated. + indicates growth after 5 days at 24 °C. *0* indicates no growth after 5 days at 24 °C. *D*, Arm domains in Vac8p are required for Cvt transport. *vac8*Δ cells were transformed with plasmids containing either wild type *VAC8* (*WT*) or the indicated arm deletions of *VAC8*. Cells were grown overnight in SMD, and API was examined by immunoblot.

tified from the screen was found to contain part of the open reading frame corresponding to *APG13* (Fig. 1*A*). The *APG13* gene was identified as being required for macroautophagy (16) and was subsequently shown to be needed for import of prAPI (5).

To determine the domain of Apg13p that interacts with Vac8p, a series of deletions was constructed in the *APG13* gene that was used as the prey plasmid for the two-hybrid interaction. *APG13* constructs lacking the sequence for the C-terminal 46 amino acids showed a dramatically reduced interaction with a full-length *VAC8* bait plasmid (Fig. 1*B*). Conversely, an *APG13* prey construct encoding only the C-terminal 46 amino acids of Apg13p also was unable to promote interactions with Vac8p. These results suggest that the C terminus of Apg13p, including but possibly extending beyond the final 46 amino acids, is required for the interaction. However, additional data suggest that more than one domain of Apg13p may be involved in the interaction with Vac8p. Apg13p lacking amino acids 568 to 738 is able to partially complement the prAPI import defect of an *apg13*Δ strain.[2] The truncated Apg13 protein does not function as efficiently as full-length Apg13p, suggesting that the absence of the interaction domain causes a kinetic defect in prAPI import.

The bulk of the structure of Vac8p consists of 11 consecutive armadillo (Arm) repeats, each of 40–42 amino acids in length. These domains are thought to mediate protein-protein interactions (26). To determine if the interaction of Vac8p and Apg13p depends on the presence of Arm repeats within Vac8p, we tested the effect of deleting various Vac8p Arm domains by two-hybrid analysis. We found that, with the exception of Arm 1, all the Arm repeats examined were required for detection of the Vac8p-Apg13p interaction by the two-hybrid method (Fig. 1*C*). All of these Vac8p Arm deletion constructs produce stable proteins in yeast (data not shown). Next, we examined the effect of the Arm deletions on transport of prAPI. By immunoblot analysis, with the exception of the Arm 1 deletion, prAPI accumulated in cells where the only Vac8p present contained an Arm deletion (Fig. 1*D*). The fact that mutations that appear to prevent interaction of Vac8p and Apg13p also inhibit Cvt transport suggests that the Arm domains are important for Vac8p function. Furthermore, these results suggest that the interaction between Vac8p and Apg13p is needed for efficient import of prAPI through the Cvt pathway.

To verify that the native Vac8 and Apg13 proteins interact *in vivo*, we performed a co-immunoprecipitation analysis. Protein extracts were prepared from yeast cells under native conditions and immunoprecipitated with antiserum to Vac8p. The immunoprecipitates were resolved by SDS-polyacrylamide gel electrophoresis, transferred to polyvinylidene fluoride membrane, and Apg13p was detected by immunoblot using anti-Apg13p

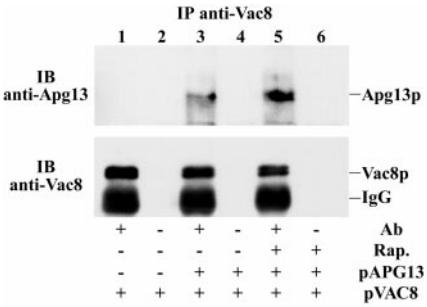

FIG. 2. **Biochemical interaction between Vac8p and Apg13p.** Cells overexpressing Vac8p were subjected to native immunoprecipitation with or without anti-Vac8p antiserum as described under "Experimental Procedures." The immunoprecipitated sample was then subjected to immunoblotting with antiserum against Apg13p and Vac8p. Cells contained overexpressed Apg13p (pAPG13) as indicated. Addition of rapamycin (*Rap*.) to the cultures is indicated.

antiserum as described under "Experimental Procedures." When the immunoprecipitation was carried out in a strain overexpressing *VAC8*, but with a deletion in the chromosomal *APG13* locus, only Vac8p was detected on the immunoblot, indicating that there were no background bands that migrated at the position of Apg13p (Fig. 2, *lane 1*). Similarly, in the absence of antiserum to Vac8p, neither protein was detected on the immunoblot, indicating that they did not bind nonspecifically to the protein G-Sepharose beads (Fig. 2, *lanes 2*, *4*, and *6*). In contrast, Apg13p was found to co-immunoprecipitate with anti-Vac8p antiserum when both Vac8p and Apg13p were expressed from multicopy plasmids (Fig. 2, *lane 3*). This result confirms that Vac8p and Apg13p interact *in vivo*. The drug rapamycin mimics starvation conditions and induces autophagy by inhibiting the Tor kinase (27). Apg13p and Vac8p were found to interact *in vivo* following treatment with rapamycin (Fig. 2, *lane 5*). Similarly, Vac8p and Apg13p were found to interact under starvation conditions based on the two-hybrid analysis (data not shown). These results mean that Vac8p and Apg13p interact under both vegetative conditions where the Cvt pathway functions and starvation conditions that induce autophagy.

Both genetic and biochemical data indicate that Apg13p interacts with another protein required for both the Cvt pathway and autophagy, the serine/threonine kinase Apg1p (16, 28),[2] In addition, recent two-hybrid results showing that Apg13p and Apg1p interact corroborate these findings (29). The Vac8p/Apg13p interaction was not dependent on the presence of Apg1p because similar two-hybrid results were obtained in an *apg1*Δ strain (Fig. 1*A*). These result suggest that Vac8p and Apg13p interact independent of Apg1p.

Strains with Mutations in VAC8 and APG13 Are Defective in the Membrane Enwrapping Step of the Cvt Pathway—Biochemical localization of prAPI has been used to determine the step of the Cvt pathway that is blocked in various *apg* and *cvt* mutants (10). Mutants that are blocked in vesicle formation accumulate Cvt complexes, indicated by the appearance of prAPI in a low speed pellet fraction. Flotation analyses demonstrate whether the Cvt complex is associated with membrane. Protease protection assays distinguish between prAPI trapped in a Cvt complex that is not fully surrounded by membrane and is therefore protease-accessible in permeabilized cells, and prAPI trapped in Cvt vesicles that appears protease-protected. Further biochemical fractionation of mutants that accumulate protease-protected prAPI demonstrates whether prAPI is contained within cytosolic vesicles (Cvt vesicles) or subvacuolar vesicles (Cvt bodies). By these analyses, Apg5p, Apg7p, Apg9p, and Aut7p have been shown to affect Cvt vesicle formation/completion (30–33); Vam3p, Ypt7p, and Vps18p are required for Cvt vesicle fusion (10, 31, 34); and Cvt17p is required for the breakdown of Cvt bodies within the vacuole (10).

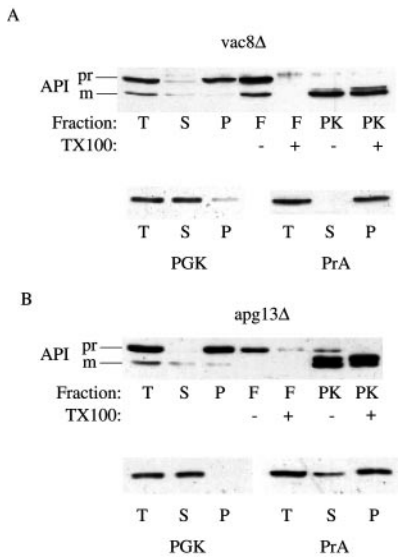

FIG. 3. **Precursor API in *vac8*Δ and *apg13*Δ strains is membrane-associated but not enclosed within completed vesicles.** Isolated spheroplasts from either the *vac8*Δ strain (D3Y102) *A*, or the *apg13*Δ strain (D3Y101) *B*, were osmotically lysed and the total fraction (*T*) was separated into a supernatant (*S*) and pellet (*P*) fraction by centrifugation. The resulting fractions were subjected to immunoblotting with antiserum against API, PrA (a vacuole lumenal marker), or PGK (a cytosolic marker). The pellet fraction was further analyzed by flotation through Ficoll step gradients, resulting in the float (*F*) fraction. 1% Triton X-100 was either added to (+) or omitted from (−) the pellet fraction before separation on the gradient. The lysed total fraction was subjected to proteinase K treatment (*PK*) either in the absence (−), or presence (+) of 0.2% Triton X-100 as described under "Experimental Procedures." The positions of precursor (*pr*) and mature (*m*) API are indicated. Note that prAPI is digested to the mature size by proteinase K.

We examined the state of prAPI to determine the step of the Cvt pathway that is blocked in the *vac8* and *apg13* mutants. Spheroplasts isolated from either *vac8*Δ or *apg13*Δ strains were subjected to differential osmotic lysis under conditions that have been shown to efficiently lyse the plasma membrane while preserving the integrity of most vacuoles (4, 23, 35). These permeabilized spheroplasts were then separated into pellet and supernatant fractions by centrifugation at 5000 × *g*. In both mutant strains, the majority of prAPI was found in the pellet fraction (Fig. 3, *A* and *B*). We examined the localization of the vacuolar hydrolase PrA and the cytosolic protein PGK in the same samples as controls for the fractionation. The majority of PGK was recovered in the supernatant fraction, while PrA was found in the pellet fraction, indicating that the fractionation was successful (Fig. 3, *A* and *B*).

To determine if the prAPI recovered in the pellet fraction was in fact associated with membrane components, we performed a flotation analysis using the pellet fraction as the starting material. The prAPI trapped in both the *vac8*Δ and *apg13*Δ strains floated through a Ficoll gradient in the absence, but not in the presence, of detergent, suggesting that this population of prAPI is membrane-associated. It is possible that flotation of prAPI under these conditions reflects binding to lipid rather than a membrane bilayer. However, in an *apg5*^{ts} mutant we were able to verify through electron microscopy that flotation of prAPI corresponded with membrane association (30). When permeabilized cells from the *vac8*Δ and *apg13*Δ strains were examined by protease treatment, the majority of prAPI was accessible to added protease in both the presence

and absence of detergent (Fig. 3, *A* and *B*). Because the vacuolar hydrolase PrA is primarily recovered in the pellet fraction, intracellular compartments such as vacuoles (which are one of the most osmotically labile subcellular compartments) are intact in these samples. These results suggest that prAPI is localized in a membrane-associated Cvt complex, and that Vac8p and Apg13p are required for formation of the fully membrane enclosed Cvt vesicle.

Vac8p Is Not Essential for Autophagy—We have reported previously that autophagic bodies are detected in *vac8*Δ cells by light microscopy, and thus Vac8p appeared not to be required for autophagy (12). Because the majority of molecular components are shared between the Cvt and autophagy pathways, we further investigated the role of Vac8p in autophagy. Precursor API is transported by the Cvt pathway in nutrient-rich conditions and by the autophagy pathway in starvation conditions (3, 5). Accordingly, we examined the kinetics of prAPI maturation in different nutritional conditions as a biochemical method of examining the autophagy defect in the *vac8*Δ and *apg13*Δ strains. In wild type cells, prAPI is matured with a half-time of about 30 min in both SMD and SD-N media (Fig. 4*A*). In contrast, in an *apg1*Δ strain, no mature API is detected in either nutrient condition. In *apg13*Δ cells, API maturation is essentially completely blocked in YPD medium (data not shown). In contrast, some mature API is detected after a 90-min chase in SMD medium. When these cells are chased in SD-N, about 70% of API is mature at the 90-min chase point (Fig. 4*B*). In *vac8*Δ cells, prAPI delivery is negligible in nitrogen-containing medium, and restored to near wild type levels in starvation medium. These results suggest that prAPI can be efficiently transported by autophagy in *vac8*Δ cells during starvation, and that Vac8p has a more central role in the Cvt pathway than in the autophagy pathway. Furthermore, the defect in prAPI import in the *apg13*Δ strain can be partially overcome under starvation conditions.

To examine the kinetics of autophagy in these mutants directly, we utilized an alkaline phosphatase construct that was designed as a marker for the autophagy pathway (36). This protein, called Pho8Δ60p, consists of alkaline phosphatase in which the membrane-spanning region and the vacuole targeting information have been deleted (18, 37). The resulting cytosolic protein is only delivered to the vacuole when autophagy is induced. Pho8Δ60p still contains a site for cleavage of the C-terminal propeptide by the vacuole hydrolase proteinase B. Therefore, vacuolar delivery of Pho8Δ60p results in cleavage to a lower molecular weight species, and activation of enzyme activity. A pulse-chase experiment was performed to compare the kinetics of the autophagic uptake of Pho8Δ60p in wild type, *vac8*Δ, and *apg13*Δ cells (Fig. 4*C*). In wild type cells, maturation of Pho8Δ60p proceeds rapidly to about the 8-h chase point and then plateaus at about 18% delivery. In contrast, the *apg13*Δ strain matures only a very low level of Pho8Δ60p, consistent with its classification as an autophagy mutant. In *vac8*Δ cells, an intermediate level of Pho8Δ60p maturation was observed, suggesting that the autophagy pathway is active but is not as efficient as in wild type cells.

To confirm that the autophagy pathway is carried out in *vac8*Δ cells, we examined these cells directly by electron microscopy. Autophagy results in the delivery of an intact vesicle called an autophagic body to the vacuole lumen. In cells deficient in PrA, these vesicles cannot be broken down and accumulate in starvation conditions (38). We examined the effect of the *vac8* and *apg13* deletions on vesicle accumulation in cells in which *PEP4*, the gene encoding PrA, had been deleted. In *pep4*Δ cells after incubation in starvation conditions for 4 h, numerous autophagic bodies were detected in the vacuole (Fig. 5*A*). In the *apg13*Δ *pep4*Δ double mutant, the vacuoles appeared empty as expected, confirming a block in autophagy resulting from the *apg13* mutation (Fig. 5*B*). In contrast, in the *vac8*Δ *pep4*Δ double mutant, autophagic bodies appeared to be as abundant as in the *pep4*Δ cells (Fig. 5, compare *A* to *C*). Cells lacking Vac8p have been shown to have fragmented vacuoles (12). This was apparent in many of our images, which contained multilobed or vesiculated vacuoles containing subvacuolar vesicles (data not shown). These results confirm that autophagy proceeds in the *vac8*Δ strain.

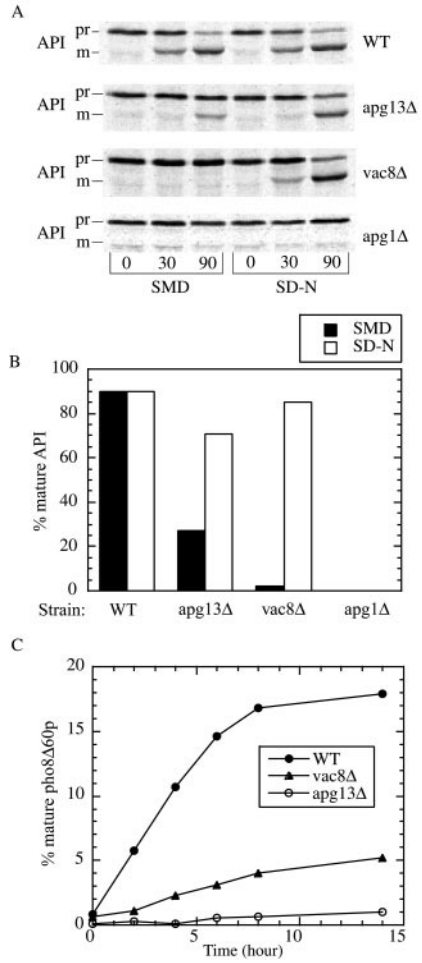

FIG. 4. **Kinetics of transport by the Cvt and autophagy pathways in *vac8*Δ and *apg13*Δ cells.** *A*, cells from the indicated strains (WT, TN121; *apg13*Δ, D3Y103; *vac8*Δ, D3Y104; *apg1*Δ, NNY20) were metabolically labeled for 10 min as described under "Experimental Procedures." After labeling, the cells were reisolated and resuspended in either SMD or SD-N and chased for the indicated times (min). API was recovered by immunoprecipitation. Note that the band running slightly below the position of mature API in the *apg1*Δ strain is a background band. The positions of precursor (*pr*) and mature (*m*) API are indicated. *B*, quantitation of the 90-min time point of the samples in *A* are depicted. The *black bars* represent the SMD chase, and the *white bars* the SD-N chase. The amount of mature API in the *apg1*Δ strain in either condition was less than 1%. *C*, kinetics of Pho8Δ60p delivery. Cells (wild type, TN121; *vac8*Δ, D3Y104; *apg13*Δ, D3Y103) were metabolically labeled for 10 min in nitrogen-containing medium, washed, and chased for the indicated times in SD-N. Pho8Δ60p was recovered by immunoprecipitation with anti-ALP antiserum, resolved by SDS-polyacrylamide gel electrophoresis, and quantified using a STORM PhosphorImager (Molecular Dynamics, Sunnyvale, CA).

Vac8p Is a Phosphoprotein—Apg13p is a phosphoprotein that interacts with Apg1p.[2] Although Apg1p is both a phosphoprotein and a protein kinase (28), the phosphorylation of Apg13p does not appear to depend on Apg1p (Fig. 6*C*). To determine if Vac8p is also a phosphoprotein, cells were meta-

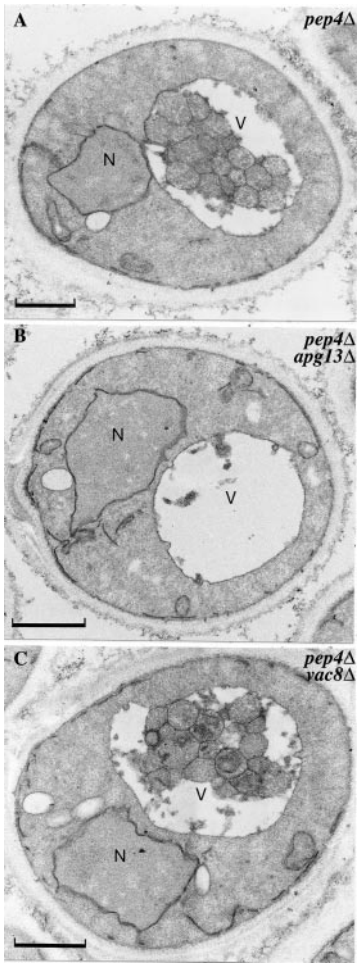

FIG. 5. **Electron microscopy of *vac8*Δ and *apg13*Δ cells reveals that *vac8*Δ cells are competent for autophagy.** *A–C*, TVY1 (*A*; *pep4*Δ), D3Y105 (*B*; *apg13*Δ *pep4*Δ), and D3Y106 (*C*; *pep4*Δ *vac8*Δ) cells were grown to log phase in YPD and then shifted to SD-N for 4 h before fixation with potassium permanganate. Electron microscopy was carried out as described under "Experimental Procedures." *N*, nucleus; *V*, vacuole; *bar*, 1 μm.

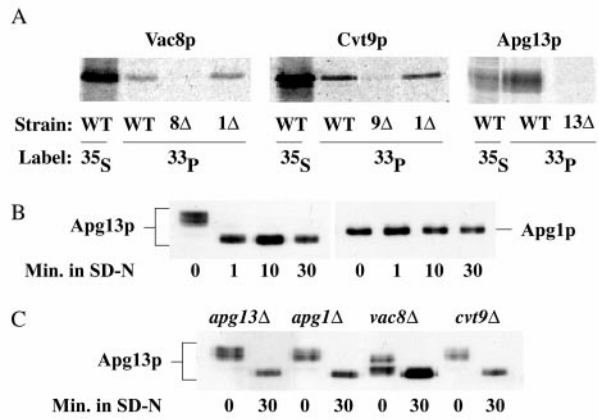

FIG. 6. *A*, Vac8p, Apg13p, and Cvt9p are phosphoproteins. Cells from the indicated strains (wild type (*WT*), SEY6210; *vac8*Δ, D3Y102; *apg1*Δ, NNY20; *cvt9*Δ, AHY001; *apg13*Δ, D3Y101) were labeled with either ^{35}S or ^{33}P and subjected to immunoprecipitation with the indicated antisera. Vac8p was expressed from the chromosomal locus, and Cvt9p and Apg13p were overexpressed. *B*, Apg13p is hyperphosphorylated in rich media. Cells deleted for either *APG13* (D3Y101) or *APG1* (NNY20) containing either overexpressed Apg13p or Apg1p, respectively, were grown in SMD and then shifted to SD-N at time 0. Samples were collected at the indicated time points, and Apg1p and Apg13p detected by immunoblotting. *C*, hyperphosphorylation of Apg13p is defective in *vac8*Δ cells. Apg13p was overexpressed in the indicated strains (*apg13*Δ, D3Y101; *apg1*Δ, NNY20; *vac8*Δ, D3Y102; *cvt9*Δ, AHY001). The cultures were grown in SMD and shifted to SD-N for either 0 or 30 min. Apg13p was detected by immunoblot.

bolically labeled with [^{33}P]orthophosphate, and Vac8p was recovered by immunoprecipitation. Labeled Vac8p was recovered from cell lysates (Fig. 6*A*), indicating that it is a phosphoprotein. In addition, the level of Vac8p phosphorylation was not changed in an *apg1*Δ strain, suggesting that Apg1p is not the kinase responsible for Vac8p phosphorylation. Apg1p also interacts with Cvt9p.[3] Like Vac8p, Cvt9p appears to play a more predominant role in Cvt transport than in the autophagy pathway. To determine if Cvt9p is phosphorylated, cells were again subjected to metabolic labeling with [^{33}P]orthophosphate, and Cvt9p was recovered by immunoprecipitation. As is the case for Apg13p and Vac8p, Cvt9p is a phosphoprotein that does not appear to depend on Apg1p for phosphorylation, despite the fact that Apg1p and Cvt9p form a complex.

The level of Apg13p phosphorylation is dependent on nutritional conditions.[2] The protein is hyperphosphorylated in rich media and undergoes partial dephosphorylation in starvation conditions. Because phosphate starvation conditions were required to get incorporation of labeled phosphate for these experiments, it was not possible to compare the level of phosphorylation in starvation and non-starvation conditions by the labeling method. However, Apg13p hyperphosphorylation results in a shift in relative mobility that we could detect by SDS-polyacrylamide gel electrophoresis and immunoblot. For these experiments, cells were grown in rich medium and then shifted to SD-N at time 0. Upon shifting to nitrogen starvation conditions, Apg13p was rapidly dephosphorylated as indicated by the presence of a lower molecular weight immunoreactive band (Fig. 6*B*). In contrast, the migration of Apg1p is not affected by the change in available nitrogen. Because migration of Apg1p is not affected by nutrient conditions, it is not possible to use this method to determine if the level of Apg1p phosphorylation is nitrogen-dependent.

We also examined other mutant strains for effects on regulation of Apg13p phosphorylation. Although most of the mutant strains we examined including *cvt9*Δ and *apg1*Δ did not alter the starvation induced dephosphorylation of Apg13p, we did detect a change in the phosphorylation pattern of Apg13p in *vac8*Δ cells (Fig. 6*C*). In wild type cells, the majority of Apg13p was present in a high molecular weight form when the cells were grown in rich media. In contrast, in *vac8*Δ cells, only about 50% of Apg13p existed in the hyperphosphorylated state in these conditions. These results suggest that hyperphosphorylation of Apg13p in rich media is impaired in the absence of Vac8p.

Apg13p and Apg1p Are Membrane-associated—Vac8p is associated with the vacuole membrane (12, 14, 15). To determine if Apg13p and Apg1p are also membrane-associated proteins, subcellular fractionation experiments were performed. Both Apg13p and Apg1p are expressed at low levels in the cell and are labile in cell lysates. In order to detect these proteins in subcellular fractionation experiments, overexpression of these proteins was necessary, and even with the addition of protease inhibitors, it was not possible to perform prolonged fractionation procedures. Spheroplasts prepared from cells overexpressing either Apg13p or Apg1p were lysed osmotically and separated into supernatant and pellet fractions. After centrifugation at 13,000 × *g*, Apg13p was recovered completely in the pellet fraction (Fig. 7*A*). As expected, Vac8p was also recovered in the pellet fraction, while the cytosolic marker PGK was recovered in the supernatant fraction, confirming that membrane and soluble proteins are effectively separated in this

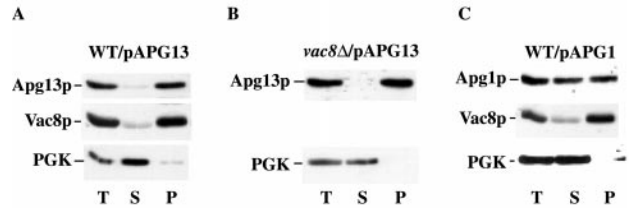

FIG. 7. **Apg13p and Apg1p are localized to a pellet fraction.** Wild type (SEY6210) (*A* and *C*) or *vac8*Δ (D3Y102) cells (*B*) containing overexpressed Apg13p (*A* and *B*) or overexpressed Apg1p (*C*) were subjected to osmotic lysis in PS200 with $MgCl_2$ and protease inhibitors. The total (*T*), supernatant (*S*), and 13,000 × *g* pellet (*P*) fractions were collected. The indicated proteins were detected by immunoblot.

experiment. Apg13p is predicted to be a soluble protein based on sequence analysis. To determine if its membrane localization is mediated through Vac8p, Apg13p fractionation was also examined in *vac8*Δ cells. As in wild type cells, Apg13p was recovered in the pellet fraction in *vac8*Δ cells, indicating it does not depend on its interaction with Vac8p for membrane localization (Fig. 7*B*). In contrast to these results, a GFP-Apg13p fusion protein displayed a diffuse cytosolic localization (data not shown). Although this fusion protein complemented the prAPI accumulation phenotype of the *apg13*Δ strain, it is possible that it has an altered subcellular distribution due to steric interference by GFP.

Apg1p is also predicted to be a soluble protein based on its deduced amino acid sequence. However, when the subcellular distribution was examined, about 50% of Apg1p was recovered in the 13,000 × *g* pellet fraction (Fig. 7*C*). As before, Vac8p and PGK were recovered primarily in the pellet and supernatant fractions, respectively. When the 13,000 × *g* supernatant fraction from these experiments was subjected to centrifugation at 100,000 × *g*, Apg1p remained in the supernatant fraction (data not shown). Because some Apg1p was degraded in this longer experiment, we cannot rule out the possibility that a fraction of Apg1p may be in the 100,000 × *g* pellet fraction. However, it appears that the bulk of Apg1p is distributed between a 13,000 × *g* pellet fraction and a soluble pool.

Because both Apg13p and Apg1p are required for autophagy, and these proteins are thought to form a more stable complex in starvation conditions,[2] localization of these proteins was also examined after incubation for 4 h in SD-N medium. This treatment did not affect the localization of either protein. Apg13p was still recovered in the 13,000 × *g* pellet fraction, and Apg1p was distributed between the supernatant and pellet fractions (data not shown).

DISCUSSION

Vac8p is required for vacuole inheritance and Cvt transport. Vac8p contains 11 armadillo (Arm) repeats. This structural domain has been found in a number of proteins with diverse functions and may serve as a scaffold for protein-protein interactions (26). Two-hybrid analysis and co-immunoprecipitation experiments demonstrate that Vac8p and Apg13p physically interact with each other, and this interaction appears to be mediated through Arm domains in Vac8p (Figs. 1 and 2). A C-terminal domain of Apg13p in the context of a two-hybrid protein was shown to be required for interaction with a corresponding Vac8p two-hybrid construct. Surprisingly, deletion of this domain in native Apg13p still allowed the truncated protein to partially complement the Cvt pathway defect in an *apg13*Δ strain. One explanation may be the presence of additional sites in Apg13p that allow interaction with Vac8p. These sites may not be functional in the context of the two-hybrid protein. A similar situation may be seen with the GFP-Apg13p hybrid protein that displays a subcellular distribution distinct from that of the native Apg13 protein, *i.e.* fusions to Apg13p may in some cases interfere with its ability to interact with other proteins. Both native Vac8p and Apg13p are membrane-associated. For Apg13p, membrane binding is independent of Vac8p (Fig. 7). The ability to bind the target membrane may allow the truncated Apg13p to interact inefficiently with Vac8p due to a close proximity even in the absence of the C-terminal Vac8p-binding domain. Alternatively, it is possible that the truncated Apg13p does not bind Vac8p but is able to function in the Cvt pathway through its interaction with other components. Subcellular fractionation experiments demonstrate that prAPI, the only known cargo of the Cvt pathway, is trapped in a membrane-bound, protease-accessible state in both the *vac8*Δ and *apg13*Δ strains, suggesting that both proteins are required for the formation/completion of Cvt vesicles (Fig. 3).

Vac8p has several cellular roles and appears to be an abundant protein compared with other identified autophagy components. Other Arm proteins such as β-catenin/armadillo also exert multiple functions through interaction with different binding partners. The crystal structure of β-catenin has been solved (39). The Arm repeats form a single rod-like structure with a hydrophobic core. Each Arm domain folds into three α-helical segments connected by short spacers. These helices are then packed into a superhelical structure with a positively charged groove that is thought to form a surface for interaction with other proteins.

Vac8p is primarily located on the vacuole and requires acylation for both correct localization and its role in vacuole inheritance (12). The fact that Vac8p acylation is not required for Cvt transport suggests that a different subset of the Vac8p population may be utilized for Cvt transport (12). This population of Vac8p is likely to be in a complex with Apg13p and bound to a membrane fraction that may or may not be the vacuole. In addition, other components such as Cvt9p that may interact, perhaps indirectly, with Vac8p appear to be located in proximity to the vacuole.[3] Given the protease-sensitive, membrane-associated phenotype of prAPI in the *vac8* null strain, it is also possible that Vac8p associates with the Cvt vesicle and is required for a fusion step that results in vesicle completion.

Vac8p and Apg13p are part of the same protein complex that includes Apg1p and Cvt9p.[3] However, the respective mutant strains display somewhat different phenotypes (Figs. 4 and 5). The *apg1*Δ strain is completely blocked in autophagy and prAPI import in rich media or starvation conditions. In synthetic minimal medium containing nitrogen, *apg13*Δ cells slowly mature prAPI and the level of import is increased in medium lacking nitrogen. However, the *apg13*Δ strain is defective for autophagy, as assessed both morphologically and by maturation of Pho8Δ60p. The *vac8*Δ strain is completely blocked for prAPI import in YPD or SMD. In contrast, in SD-N this strain shows import kinetics that only slightly lag behind those of the wild type strain. Similarly, the *vac8*Δ cells appear to carry out autophagy in SD-N medium although at a substantially reduced rate.

One explanation for these results is that Vac8p is specific to the Cvt pathway. Accordingly, the induction of autophagy allows efficient import of prAPI in the *vac8*Δ strain. The partial defect in autophagy seen in the *vac8*Δ strain could be an indirect effect of the null mutation or might be due to an alteration in the state of the interacting protein Apg13p. It is also possible that Vac8p plays a role in autophagosome formation but is not essential for this process so that *vac8*Δ cells display only a kinetic defect in autophagy. The *apg13*Δ cells may carry out autophagy at a level that is too low to detect based on delivery of Pho8Δ60p or electron microscopy. However, this level of autophagy may be sufficient to account for the selective import

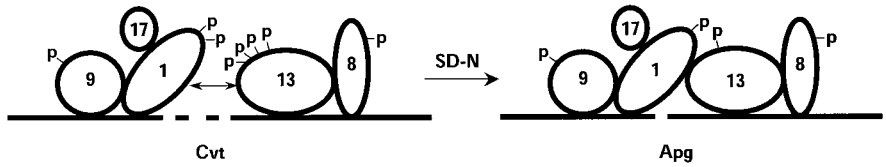

FIG. 8. **Model for interactions among Vac8p, Apg13p, Apg1p, Apg17p, and Cvt9p.** In rich media conditions that support transport by the Cvt pathway, Vac8p and Apg13p form a protein complex and Apg13p is hyperphosphorylated. In starvation conditions (SD-N), the autophagy pathway is activated, the phosphorylation of Apg13p is reduced, and Apg1p binds Apg13p more tightly. Proteins are indicated by *number* as follows: Apg1p, *1*; Apg13p, *13*; Apg17p, *17*; Cvt9p, *9*; Vac8p, *8*. Additional proteins may also be present in this complex. Phosphorylation is indicated by *p*. The phosphorylation state of Apg17p was not determined.

of prAPI observed in our experiments. An alternative explanation is afforded by the observation that the *apg13* mutant is leaky for the Cvt pathway in nitrogen-containing SMD medium. This mutant may carry out transport of prAPI through the formation of Cvt vesicles during both vegetative and starvation conditions. Because Cvt vesicles are of comparatively low abundance, they may not have been detected by our electron microscopy analysis. Finally, it is possible that Apg13p is required for both pathways but like Vac8p it can be bypassed. For example, overexpression of Apg1p suppresses the *apg13–1* mutation (16).

Vac8p and Apg13p, the Apg13p-interacting protein Apg1p, and the Apg1p-interacting protein Cvt9p are phosphorylated *in vivo* (Fig. 6). Apg13p and Cvt9p are thought to interact directly with Apg1p, which is proposed to be a protein kinase. However, these proteins are phosphorylated in *apg1*Δ cells, suggesting that another kinase is involved. Apg13p is hyperphosphorylated in rich media conditions; when cells are shifted to a poor nitrogen source, it is rapidly dephosphorylated (Fig. 6*B*). This nutrient-dependent change in the level of Apg13p phosphorylation could signal the change from transport via the Cvt pathway to the macroautophagy pathway. Hyperphosphorylation of Apg13p is reduced in *vac8*Δ cells (Fig. 6*C*), suggesting that the Vac8p/Apg13p complex may be a better substrate for phosphorylation than Apg13p alone and that Vac8p may help regulate Apg13p hyperphosphorylation.

Both Apg13p and Apg1p are predicted to be soluble proteins based on sequence analysis. In addition, a fusion protein where the first 32 amino acids of Apg1p/Aut3p were replaced with GFP appeared to be cytosolic (40). However, because this protein did not complement the autophagy defect in *apg1*Δ cells, it may not represent the localization pattern of authentic Apg1p. Similarly, a GFP-Apg13p fusion protein displayed a cytosolic fluorescence pattern, although in this case the protein was functional in the Cvt pathway (data not shown). Our fractionation experiments examining the native proteins expressed from multicopy plasmids indicate that Apg13p is localized in the P13 fraction, while Apg1p is distributed between a soluble fraction and the P13 fraction (Fig. 7). Both Apg1p and Apg13p are unstable during subcellular fractionation procedures and are present at low levels in the cell. To facilitate detection, these proteins were overexpressed. In the case of Apg1p, this may have resulted in the saturation of an Apg1p membrane binding site(s), resulting in the observed soluble pool. Alternatively, Apg1p may cycle between pools both on and off the membrane. The localization of Apg13p and Apg1p to the P13 fraction is consistent with their localization to either the vacuole, a forming Cvt vesicle, or possibly the PVC.

In our current model (Fig. 8), Apg13p and Vac8p may be part of a larger protein complex that includes Apg1p, and Cvt9p, and may include additional proteins; recently, Apg17p was found to interact with Apg1p.[2] Apg13p, Vac8p, Apg1p (28), and Cvt9p are all phosphorylated proteins, and the level of Apg13p phosphorylation is regulated by the availability of nitrogen. Apg13p and Vac8p are found in a protein complex in rich media as well as in the presence of rapamycin (Fig. 2). Apg13p and Apg1p interact more tightly in starvation conditions when Apg13p is in the lower phosphorylation state.[2] The change in the level of Apg13p phosphorylation may allow additional Apg1p and associated proteins such as Cvt9p to be recruited to the Apg13p/Vac8p complex. This event may, in turn, be involved in switching from the Cvt pathway to autophagy.

Acknowledgments—We thank Fusheng Tang, Ting Liu, and Dr. Yong-Xu Wang for construction of plasmids containing wild type and mutant forms of *VAC8* and members of the Klionsky and Weisman laboratories for helpful discussion.

REFERENCES

1. Scott, S. V., and Klionsky, D. J. (1998) *Curr. Opin. Cell Biol.* **10,** 523–529
2. Kim, J., Scott, S. V., Oda, M. N., and Klionsky, D. J. (1997) *J. Cell Biol.* **137,** 609–618
3. Baba, M., Osumi, M., Scott, S. V., Klionsky, D. J., and Ohsumi, Y. (1997) *J. Cell Biol.* **139,** 1687–1695
4. Harding, T. M., Morano, K. A., Scott, S. V., and Klionsky, D. J. (1995) *J. Cell Biol.* **131,** 591–602
5. Scott, S. V., Hefner-Gravink, A., Morano, K. A., Noda, T., Ohsumi, Y., and Klionsky, D. J. (1996) *Proc. Natl. Acad. Sci. U. S. A.* **93,** 12304–12308
6. Harding, T. M., Hefner-Gravink, A., Thumm, M., and Klionsky, D. J. (1996) *J. Biol. Chem.* **271,** 17621–17624
7. Thumm, M., Egner, R., Koch, M., Schlumpberger, M., Straub, M., Veenhuis, M., and Wolf, D. H. (1994) *FEBS Lett.* **349,** 275–280
8. Tsukada, M., and Ohsumi, Y. (1993) *FEBS Lett.* **333,** 169–174
9. Klionsky, D. J., and Ohsumi, Y. (1999) *Annu. Rev. Cell. Dev. Biol.* **15,** 1–32
10. Scott, S. V., Baba, M., Ohsumi, Y., and Klionsky, D. J. (1997) *J. Cell Biol.* **138,** 37–44
11. Abeliovich, H., Darsow, T., and Emr, S. D. (1999) *EMBO J.* **18,** 6005–6016
12. Wang, Y. X., Catlett, N. L., and Weisman, L. S. (1998) *J. Cell Biol.* **140,** 1063–1074
13. Wang, Y. X., Zhao, H., Harding, T. M., Gomes de Mesquita, D. S., Woldringh, C. L., Klionsky, D. J., Munn, A. L., and Weisman, L. S. (1996) *Mol. Biol. Cell* **7,** 1375–1389
14. Fleckenstein, D., Rohde, M., Klionsky, D. J., and Rüdiger, M. (1998) *J. Cell Sci.* **111,** 3109–3118
15. Pan, X., and Goldfarb, D. S. (1998) *J. Cell Sci.* **111,** 2137–2147
16. Funakoshi, T., Matsuura, A., Noda, T., and Ohsumi, Y. (1997) *Gene* (*Amst.*) **192,** 207–213
17. Klionsky, D. J., Banta, L. M., and Emr, S. D. (1988) *Mol. Cell. Biol.* **8,** 2105–2116
18. Klionsky, D. J., and Emr, S. D. (1989) *EMBO J.* **8,** 2241–2250
19. Baum, P., Thorner, J., and Honig, L. (1978) *Proc. Natl. Acad. Sci. U. S. A.* **75,** 4962–4966
20. Harper, J. W., Adami, G. R., Wei, N., Keyomarsi, K., and Elledge, S. J. (1993) *Cell* **75,** 805–816
21. James, P., Halladay, J., and Craig, E. A. (1996) *Genetics* **144,** 1425–1436
22. Bai, C., and Elledge, S. (1997) *Methods Enzymol.* **283,** 141–156
23. Scott, S. V., and Klionsky, D. J. (1995) *J. Cell Biol.* **131,** 1727–1735
24. Klionsky, D. J., Cueva, R., and Yaver, D. S. (1992) *J. Cell Biol.* **119,** 287–299
25. Erdmann, R., Veenhuis, M., Mertens, D., and Kunau, W. H. (1989) *Proc. Natl. Acad. Sci. U. S. A.* **86,** 5419–5423
26. Hatzfeld, M. (1999) *Int. Rev. Cytol.* **186,** 179–224
27. Noda, T., and Ohsumi, Y. (1998) *J. Biol. Chem.* **273,** 3963–3966
28. Matsuura, A., Tsukada, M., Wada, Y., and Ohsumi, Y. (1997) *Gene* (*Amst.*) **192,** 245–250
29. Uetz, P., Giot, L., Cagney, G., Mansfield, T. A., Judson, R. S., Knight, J. R., Lockshon, D., Narayan, V., Srinivasan, M., Pochart, P., Qureshi-Emili, A., Li, Y., Godwin, B., Conover, D., Kalbfleisch, T., Vijayadamodar, G., Yang, M., Johnston, M., Fields, S., and Rothberg, J. M. (2000) *Nature* **403,** 623–627
30. George, M. D., Baba, M., Scott, S. V., Mizushima, N., Garrison, B. S., Ohsumi, Y., and Klionsky, D. J. (2000) *Mol. Biol. Cell* **11,** 969–982
31. Kim, J., Dalton, V. M., Eggerton, K. P., Scott, S. V., and Klionsky, D. J. (1999) *Mol. Biol. Cell* **10,** 1337–1351
32. Huang, W.-P., Scott, S. V., Kim, J., and Klionsky, D. J. (2000) *J. Biol. Chem.* **275,** 5845–5851

33. Noda, T., Kim, J., Huang, W.-P., Baba, M., Tokunaga, C., Ohsumi, Y., and Klionsky, D. J. (2000) *J. Cell Biol.* **148,** 465–479
34. Darsow, T., Rieder, S. E., and Emr, S. D. (1997) *J. Cell Biol.* **138,** 517–529
35. Oda, M. N., Scott, S. V., Hefner-Gravink, A., Caffarelli, A. D., and Klionsky, D. J. (1996) *J. Cell Biol.* **132,** 999–1010
36. Noda, T., Matsuura, A., Wada, Y., and Ohsumi, Y. (1995) *Biochem. Biophys. Res. Commun.* **210,** 126–132
37. Klionsky, D. J., and Emr, S. D. (1990) *J. Biol. Chem.* **265,** 5349–5352
38. Takeshige, K., Baba, M., Tsuboi, S., Noda, T., and Ohsumi, Y. (1992) *J. Cell Biol.* **119,** 301–311
39. Huber, A. H., Nelson, W. J., and Weis, W. I. (1997) *Cell* **90,** 871–882
40. Straub, M., Bredschneider, M., and Thumm, M. (1997) *J. Bacteriol.* **179,** 3875–3883
41. Robinson, J. S., Klionsky, D. J., Banta, L. M., and Emr, S. D. (1988) *Mol. Cell. Biol.* **8,** 4936–4948
42. Jones, E. W. (1991) *Methods Enzymol.* **194,** 428–453
43. Gerhardt, B., Kordas, T. J., Thompson, C. M., Patel, P., and Vida, T. (1998) *J. Biol. Chem.* **273,** 15818–15829